REPORT DOCUMENTATION PAGE

Form Approved OMB NO. 0704-0188

1. REPORT DATE (DD-MM-YYYY)	2. REPORT TYPE	3. DATES COVERED (From - To)
12-03-2015	Final Report	14-Sep-2012 - 13-Oct-2014

4. TITLE AND SUBTITLE
Final Report: Functionalized MEMS Sensors for Capacity-Based Residual Life Indicators

5a. CONTRACT NUMBER
W911NF-12-1-0561

5b. GRANT NUMBER

5c. PROGRAM ELEMENT NUMBER

6. AUTHORS
Peter J. Hesketh, Curtis Mowry

5d. PROJECT NUMBER

5e. TASK NUMBER

5f. WORK UNIT NUMBER

7. PERFORMING ORGANIZATION NAMES AND ADDRESSES
Georgia Tech Research Corporation
505 Tenth Street NW

Atlanta, GA 30332 -0420

8. PERFORMING ORGANIZATION REPORT NUMBER

9. SPONSORING/MONITORING AGENCY NAME(S) AND ADDRESS (ES)
U.S. Army Research Office
P.O. Box 12211
Research Triangle Park, NC 27709-2211

10. SPONSOR/MONITOR'S ACRONYM(S)
ARO

11. SPONSOR/MONITOR'S REPORT NUMBER(S)
62480-CH.4

12. DISTRIBUTION AVAILIBILITY STATEMENT
Approved for Public Release; Distribution Unlimited

13. SUPPLEMENTARY NOTES
The views, opinions and/or findings contained in this report are those of the author(s) and should not contrued as an official Department of the Army position, policy or decision, unless so designated by other documentation.

14. ABSTRACT
Technologies that provide real-time assessment of filter impregnate residual lifetime will increase the efficiency of filter usage and ensure safe operating conditions. Detection technologies that are small and can be located within or near filter elements are desirable. Low-cost devices are also necessary, since filter usage is widespread. Recognition chemistries are also required to provide both sensitivity and selectivity, since gases passing through filters may contain a wide range of components. To meet this need Sandia National Laboratories and Georgia Institute of Technology are teaming to develop microfabricated sensors for residual life indication.

15. SUBJECT TERMS
microcantilever, sensor

16. SECURITY CLASSIFICATION OF:			17. LIMITATION OF ABSTRACT	15. NUMBER OF PAGES	19a. NAME OF RESPONSIBLE PERSON
a. REPORT	b. ABSTRACT	c. THIS PAGE			Peter Hesketh
UU	UU	UU	UU		19b. TELEPHONE NUMBER 404-385-1358

Report Title

Final Report: Functionalized MEMS Sensors for Capacity-Based Residual Life Indicators

ABSTRACT

Technologies that provide real-time assessment of filter impregnate residual lifetime will increase the efficiency of filter usage and ensure safe operating conditions. Detection technologies that are small and can be located within or near filter elements are desirable. Low-cost devices are also necessary, since filter usage is widespread. Recognition chemistries are also required to provide both sensitivity and selectivity, since gases passing through filters may contain a wide range of components. To meet this need Sandia National Laboratories and Georgia Institute of Technology are teaming to develop microfabricated sensors for residual life indication.

We are studying highly sensitive microsensor platforms for residual life indication. Piezoresistive static microcantilevers respond to changes in surface stress by changing resistance as the cantilever deflects from analyte interaction with the surface coating. Sensitivity to sub-nanogram quantities are predicted. Our research focuses on the response of active sensor coatings to battlefield contaminants, and potentially interfering compounds that are otherwise of no concern.

The key achievements this year on the project have been as follows: (1) new microcantilever sensor designs were fabricated and coated with Ag and Cu thin films and delivered to Sandia for evaluation; (2) Modifications to the new flow cell was set up for multi-sensor measurements; and (3) Modeling with COMSOL indicates some interesting characteristics for front versus back side coated sensors and as a function of the reaction regions within the coatings.

Enter List of papers submitted or published that acknowledge ARO support from the start of the project to the date of this printing. List the papers, including journal references, in the following categories:

(a) Papers published in peer-reviewed journals (N/A for none)

Received Paper

TOTAL:

Number of Papers published in peer-reviewed journals:

(b) Papers published in non-peer-reviewed journals (N/A for none)

Received Paper

TOTAL:

Number of Papers published in non peer-reviewed journals:

(c) Presentations

Number of Presentations: 0.00

Non Peer-Reviewed Conference Proceeding publications (other than abstracts):

Received Paper

TOTAL:

Number of Non Peer-Reviewed Conference Proceeding publications (other than abstracts):

Peer-Reviewed Conference Proceeding publications (other than abstracts):

Received Paper

TOTAL:

Number of Peer-Reviewed Conference Proceeding publications (other than abstracts):

(d) Manuscripts

Received Paper

TOTAL:

Number of Manuscripts:

Books

Received Book

TOTAL:

Received Book Chapter

TOTAL:

Patents Submitted

Patents Awarded

Awards

Graduate Students

NAME	PERCENT_SUPPORTED	Discipline
Ilya Ellern	0.10	
Anandram	0.10	
FTE Equivalent:	**0.20**	
Total Number:	**2**	

Names of Post Doctorates

NAME	PERCENT_SUPPORTED
FTE Equivalent:	
Total Number:	

Names of Faculty Supported

NAME	PERCENT_SUPPORTED	National Academy Member
Peter J. Hesketh	0.03	
FTE Equivalent:	**0.03**	
Total Number:	**1**	

Names of Under Graduate students supported

NAME	PERCENT_SUPPORTED
FTE Equivalent:	
Total Number:	

Student Metrics

This section only applies to graduating undergraduates supported by this agreement in this reporting period

The number of undergraduates funded by this agreement who graduated during this period: 0.00

The number of undergraduates funded by this agreement who graduated during this period with a degree in science, mathematics, engineering, or technology fields:..... 0.00

The number of undergraduates funded by your agreement who graduated during this period and will continue to pursue a graduate or Ph.D. degree in science, mathematics, engineering, or technology fields:..... 0.00

Number of graduating undergraduates who achieved a 3.5 GPA to 4.0 (4.0 max scale):..... 0.00

Number of graduating undergraduates funded by a DoD funded Center of Excellence grant for Education, Research and Engineering:..... 0.00

The number of undergraduates funded by your agreement who graduated during this period and intend to work for the Department of Defense 0.00

The number of undergraduates funded by your agreement who graduated during this period and will receive scholarships or fellowships for further studies in science, mathematics, engineering or technology fields: 0.00

Names of Personnel receiving masters degrees

NAME
Total Number:

Names of personnel receiving PHDs

NAME
Total Number:

Names of other research staff

NAME	PERCENT_SUPPORTED
FTE Equivalent:	
Total Number:	

Sub Contractors (DD882)

Inventions (DD882)

Scientific Progress

see attached file

Technology Transfer

Coated cantilever sensors were delivered to Sandia National Laboratories for evaluation.

FINAL TECHNICAL REPORT

March 9th, 2015

Functionalized MEMS Sensors for Capacity-Based Residual Life Indicators

Submitted by:

Peter J. Hesketh
Georgia Institute of Technology
School of Mechanical Engineering
Atlanta, GA 30324
Telephone: (404) 385-1358
Email: peter.hesketh@me.gatech.edu

And

Curtis Mowry
Sandia National Laboratories
Albuquerque, NM
Telephone: 505-844-6271
Email: arobins@sandia.gov

Submitted to:

Greg W. Peterson
ECBC/CBR Filtration Branch
5183 Blackhawk Road, Bldg. 3549
Aberdeen Proving Ground, MD 21010
Telephone: (410) 436-9794
Email: Gregory.W.Peterson@us.army.mil

1. PROJECT AND REPORT OVERVIEW

a. Technologies that provide real-time assessment of filter impregnate residual lifetime will increase the efficiency of filter usage and ensure safe operating conditions. Detection technologies that are small and can be located within or near filter elements are desirable. Low-cost devices are also necessary, since filter usage is widespread. Recognition chemistries are also required to provide both sensitivity and selectivity, since gases passing through filters may contain a wide range of components. To meet this need Sandia National Laboratories and Georgia Institute of Technology are teaming to develop microfabricated sensors for residual life indication.

b. We are studying highly sensitive microsensor platforms for residual life indication. Piezoresistive static microcantilevers (MCL) respond to changes in surface stress by changing resistance as the cantilever deflects from analyte interaction with the surface coating. Sensitivity to sub-nanogram quantities are predicted. Our research focuses on the response of active sensor coatings to battlefield contaminants, and potentially interfering compounds that are otherwise of no concern.

c. Key achievements

1. New microcantilever sensor designs were fabricated in the clean room and characterized.
2. Instrumentation was set up to evaluate the resonant frequency and piezoresistive response of cantilevers.
3. Modifications to the new flow cell was set up for multi-sensor measurements.
4. Cantilever from Georgia Tech (GT) were sputter-coated with copper, silver and delivered to Sandia for testing.
5. Modeling with COMSOL indicates some interesting characteristics for front versus back side coated sensors and as a function of the reaction regions within the coatings.

1. Fabrication and Testing of New Sensors

The new sensor designs were fabricated in the Microelectronics Clean Room at Georgia Tech. They were inspected and tested for electrically functionality. Many working sensors are present on each wafer. Figure bellow gives some examples of sensors produced on the wafer which has a maximum of 160 die.

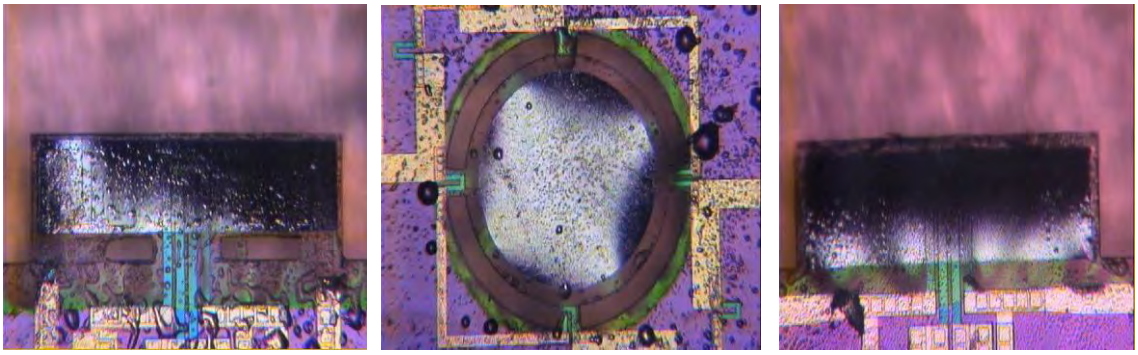

Figure 1: Three sensors, wide bridge (left), disk resonator (center) and bridge with integrated heating element (right).

The majority of the devices are wide beam design with increased sensitivity to stress in the coating. In addition, disk and narrow beam designs are included on the wafer. Some of the sensors have integrated heaters on the cantilever to assist with temperature control of the beam, when necessary. Figures above shows examples sensors from this wafer. Additional wafers have been processed with many functional sensors, approximately 160 per wafer. The majority of the devices are wide beam design with increased sensitivity to stress in the coating. In addition, disk and narrow beam designs are included on the wafer. Some of the sensors have integrated heaters on the cantilever to assist with temperature control of the beam, when necessary. Picture right shows one of the completed process wafers. Figures bellow shows examples sensors from this wafer.

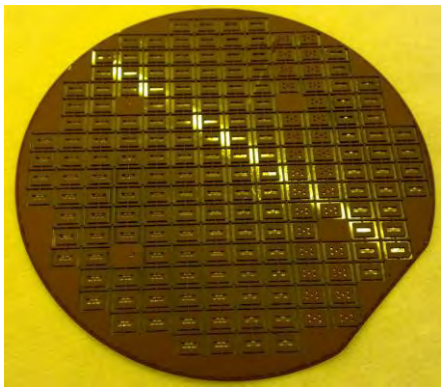

Figure 2: Optical image of completed wafer with 160 sensors.

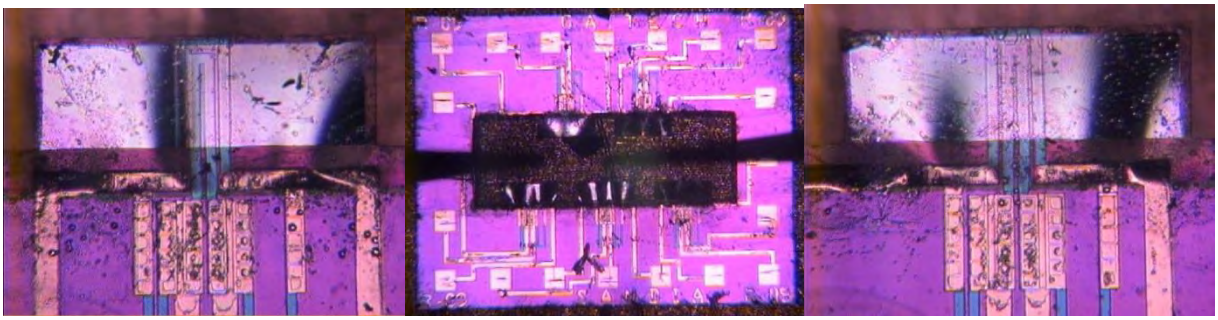

Figure 3: Images of completed working full-bridge sensors. Each die has five sensors, and they are in process of being wire bonded into packages for evaluation.

Five wafers have been processed with many functional sensors. Each die contains five sensors. The image in figure 2 shows the completed wafer. Although 95% of the cantilevers were successfully released without damage, a number of the sensors had poor electrical contacts leading to higher than expected resistance values. Bellow, figure 4, is a map of the process yield of good devices based on electrical tests. Gold indicated 80% of resistors working, Yellow indicates 60% functional, light blue indicates 40% functional and purple only one function bridge. Dark blue are nonworking, green are not yet tested, and black indicates that test structures are located in this area.

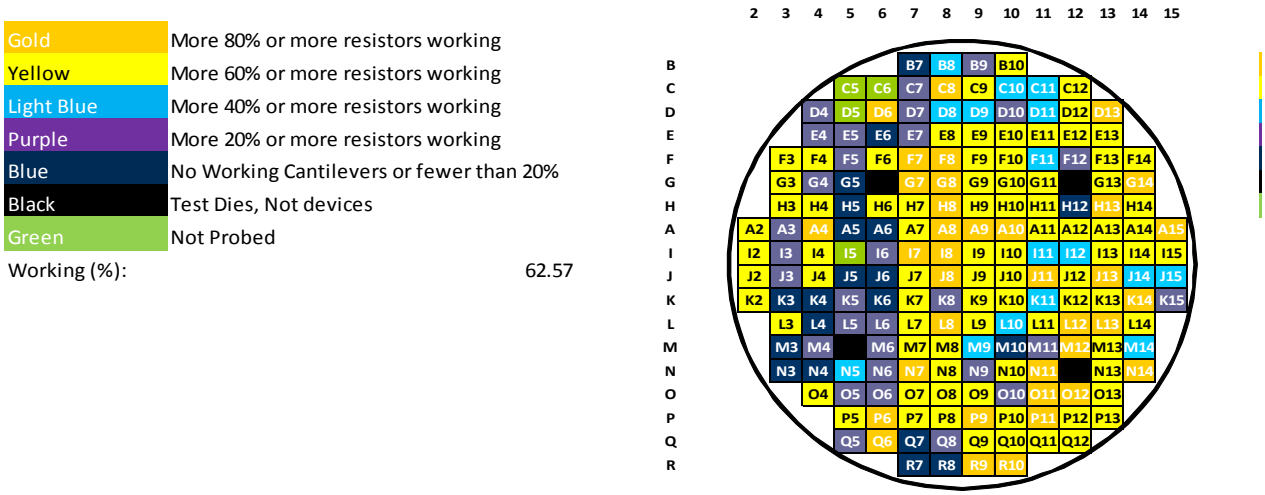

Figure 4: Yield map of process wafer number six.

Additional resistance maps were generated for each of the process wafers. The majority of the devices are wide beam design with increased sensitivity to stress of the coating. In addition, disk and narrow beam designs are included on the wafer. Some of the sensors have integrated heaters on the cantilever also.

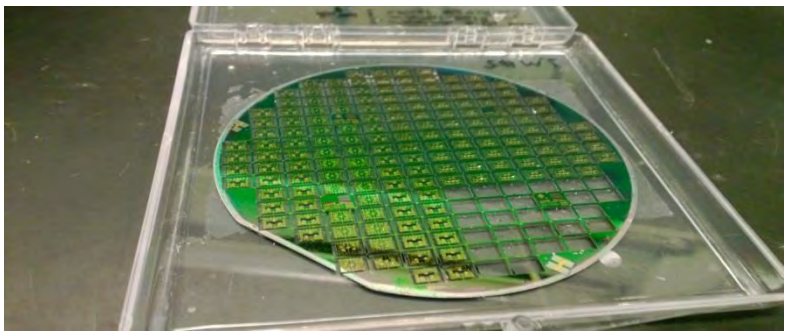

Figure 5: Photograph of completed wafer with several of the dies removed for evaluation and testing.

Characterization of Sensors

Resonant frequency of the sensors has been measured in our lab and electrical testing to determine full bridge operation. The temperature coefficient of resistance of the sensors have been determined for single sensor and in the bridge configuration, as follows: 8-10 ohms/^{o}C for stand alone, and 2-4 ohms /^{o}C with the full bridge. The use of a full bridge for the sensors is also expected to reduce noise during measurements.

Table 1: below lists examples of resistance values of sensors before and after nitride passivation coating.

Resistance (k Ohms)					
Before Nitride Deposition	After Nitride Deposition	Before Nitride Deposition	After Nitride Deposition	Before Nitride Deposition	After Nitride Deposition
2.690	2.668	3.585	3.557	3.570	3.550
2.615	2.798	3.440	3.423	3.520	3.521
2.830	2.820	3.935	3.930	10.860	10.815
2.815	2.601	10.940	10.940	3.850	3.871

The temperature coefficient of resistance was measured for example sensors in individual and full bridge connections. The temperature calibration in comparison with old sensor design is shown bellow:

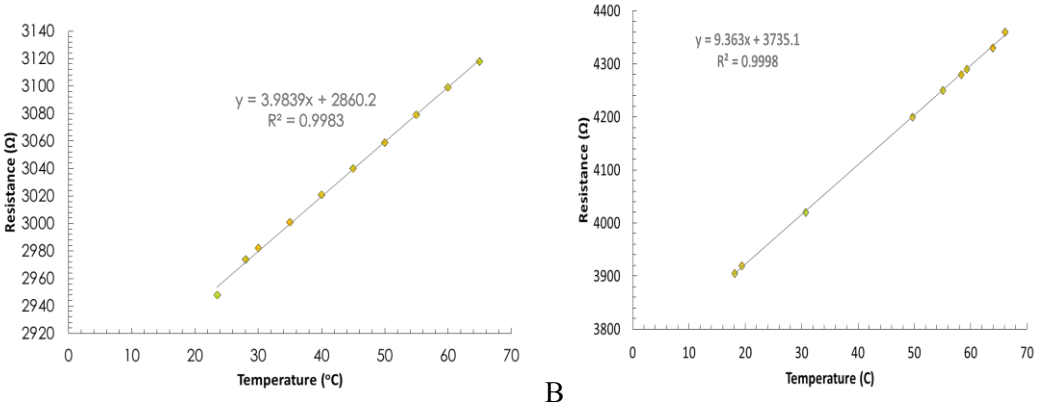

A B

Figure67: (A) Resistance versus temperature for individual sensor (narrow beam design), and (B) Resistance versus temperature for individual sensor wide beam design.

A higher temperature coefficient of resistance is observed for the new sensors because of the thin aluminum layer integrated into the cantilever to assist with the optical resonant frequency measurements. This adds to the deflection of the beam with temperature. The full bridge however has improved temperature coefficient of resistance of 2 ohms/deg C compared to the individual sensors which are 4 or 9 ohms per deg C for narrow and wide beam design, respectively.

Experiments with Sensors

Flow cell has been built for new design of cantilevers and is undergoing leak check and pressure testing. The test cell has been improved by adding additional 0-ring seal and the wiring updated to improve resolution with the bridge measurement using a lock-in-amplifier for multi-sensor testing.

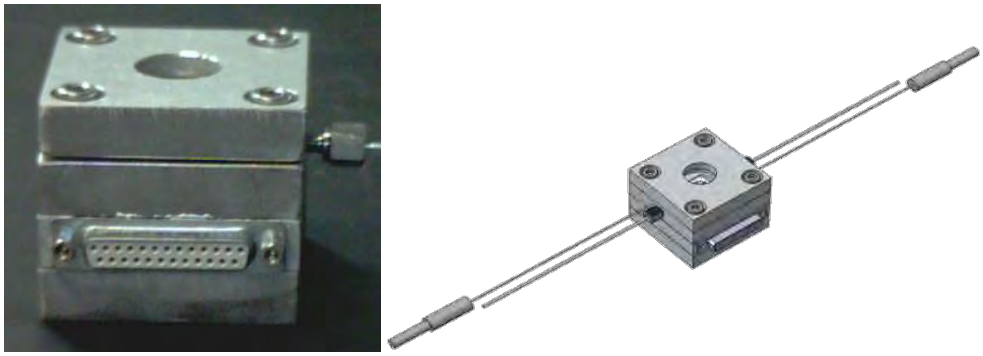

Figure 7: Photo of new sensor test cell (left) and CAD image of Sensor test cell (right).

Cantilevers were coated with Copper and Silver and delivered to Sandia Labs for evaluation. Thickness of the coatings are as follows: silver 50nm and 100nm, copper 50nm and 100nm. The sensors delivered to Sandia Laboratories with Cu and Ag coatings have been assembled into test fixture and tested with exposure to hydrogen sulfide at low concentration in dry air. The wiring was updated to improve resolution with low noise BNC cables so that the bridge measurement using a lock-in-amplifier provided for multi-sensor testing.

The new measurement cell has been built and evaluated. Sensors have been coated with MOF CuBTC films by Dr. M. Allendorf at Sandia. The sensors show improved response to surface stress generated by water vapor adsorption, compared to prior cantilever beam designs by approximately a factor of four. Testing has also been carried out with VOC's, however for some analytes only partial recovery of base-line is achieved. Therefore, the use of an AC voltage to heat the sensor to improve desorption of VOC has been investigated. A limited temperature range has been achieved with AC heating. We plan to investigate DC heating to achieve higher temperatures and improve baseline recovery.

2. Modeling of Sensors

The sensors have been modeled in COMSOL to determine the deflection and resonant frequencies. The effect of adding a heating element and including a cut-out section are being evaluated on the sensitivity and resonant frequency. Results are plotted bellow for our initial work on this modeling.

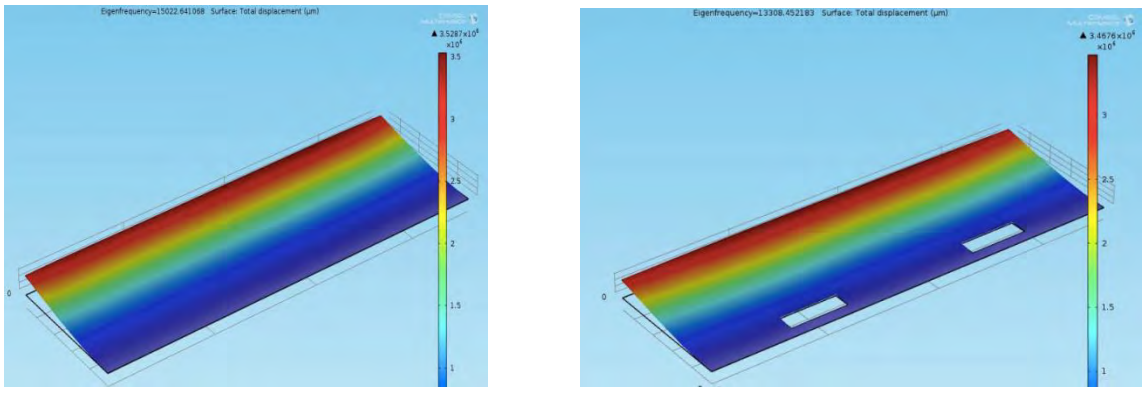

Figure 8: Plot from COMSOL of sensor deflection: without cut-outs (left) with cut-outs (right).

Table 2: Deflection and Resonant Frequency of Sensors

Mesh Count	Deflection	Frequency
408	3.619	18509.8
828	3.536	16144.1
1956	3.528	15022.6
11742	3.461	14656.5

Mesh Count	Deflection	Frequency
486	3.998	18102.6
939	3.895	167083
3816	3.477	13308.4

2.1 Front Versus Back Coating of Sensing Film

Using COMSOL 4.4 we have examined the effect of film placement and location of reaction layer on the sensor response. For a fixed chemically induced strain of 0.1% and for a Young's Modulus of 13.5GPa layer thickness 340nm, we have obtained the following results. To study of effect of strain on front coated, versus backside coated sensors the results are as follows:

Resistance (ohms)	No strain	0.1% strain	0.2% strain
Front Coating	1509.46	1452.12	1394.57
Back Coating	1509.46	1544.41	1579.20

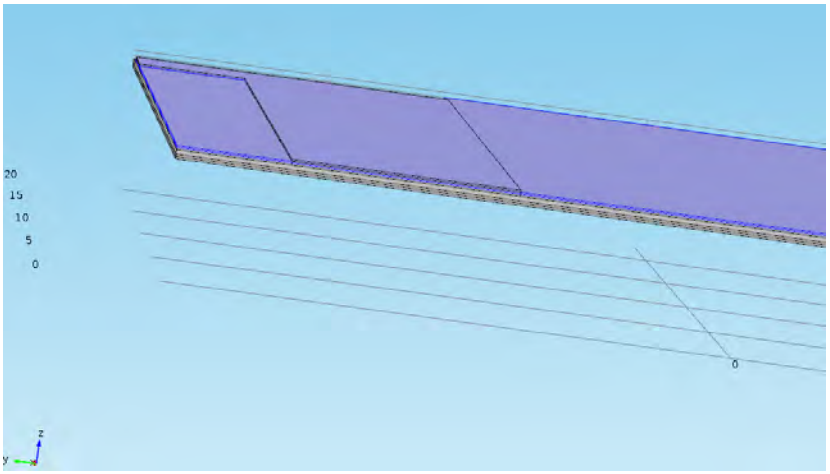

Figure 9: Image of middle section of cantilever beam showing location of piezoresistive sensor and chemical sensing film on the top which is shown in purple. Due to symmetry only one half of the sensor geometry is included in the model.

For the coating on the backside of the sensor the effect of chemically induced strain region at the surface of the sensor or at the surface of the coating was examined, by dividing the coating into two layers, one is not strained, the other section has volume induced strain of 0.1%.

Resistance (ohms)	No strain	0.1% in both layers	Strain in outer layer	Strain in inner layer
Back Coating	1509.46	1545.51	1522.28	1532.78

2.2 Effect of Sensing Film Thickness

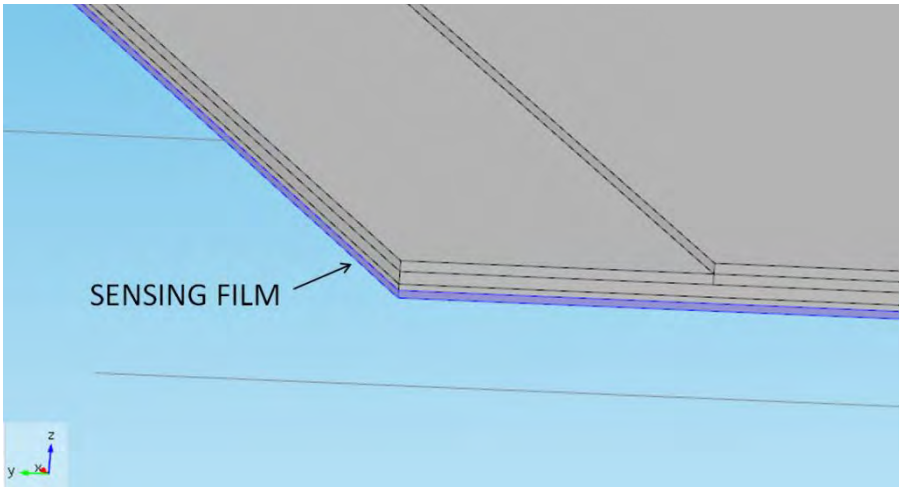

Figure 10: COMSOL screen shot showing region where chemically induced strain is produced.

The effect of the coating thickness on the back of the sensor was evaluated for the response under steady-state conditions for two different levels of strain.

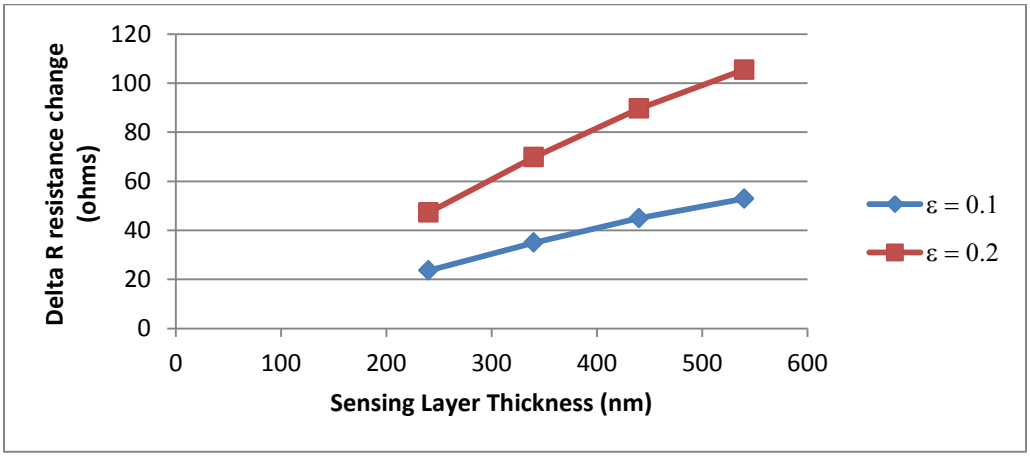

Figure 11: Plot of resistance change as a function of sensing layer thickness for two different values of chemically induced strain.

These can be compared to the effect of coating layer thickness on the front of the sensor.

2.3 Effect of Location of Chemical Strain

The placement of the reaction region along the width of the beam also has an effect on the response.

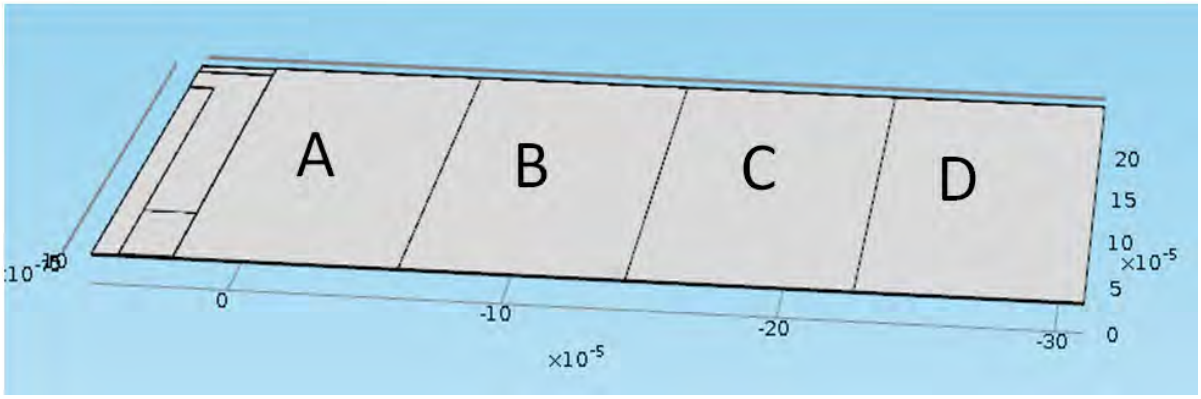

Figure 12: Image of cantilever beam showing location of different sections of the front coating of equal width. The strain can be applied to any number of these sections to examine effect of non-uniform reaction with the sensing layer.

Resistance (ohms)	Strain A only	Strain in B only	Strain in C only	Strain in D only
Front coating	1409.21	1394.30	1388.10	1445.93

The placement of strain in section B has the highest resistance response compared to section D.

Resistance (ohms)	No strain A	No strain in B	No strain in C	No strain in D
Front coating	1487.51	1481.85	1478.92	1477.20

Here the placement of the removal of strain relative to the center of the beam does not have a dramatic effect on the sensor response. These results indicate the strain is more effective closer to the surface of the cantilever beam, as one might expect.

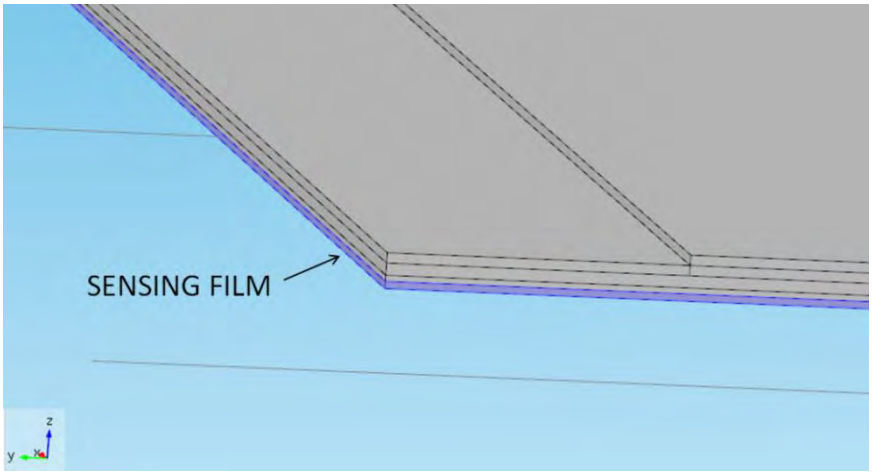

Figure 13: Image from COMSOL showing region where chemically induced strain is produced at the back of cantilever and is investigated as a function of thickness.

The effect of the coating thickness on the back of the sensor was evaluated for the response under steady-state conditions for two different levels of uniform strain in the film. Note that if this suggests a thicker film is more sensitive, but all of the film has uniform strain so a large response is generated with large chemical exposure in each case (figure 4).

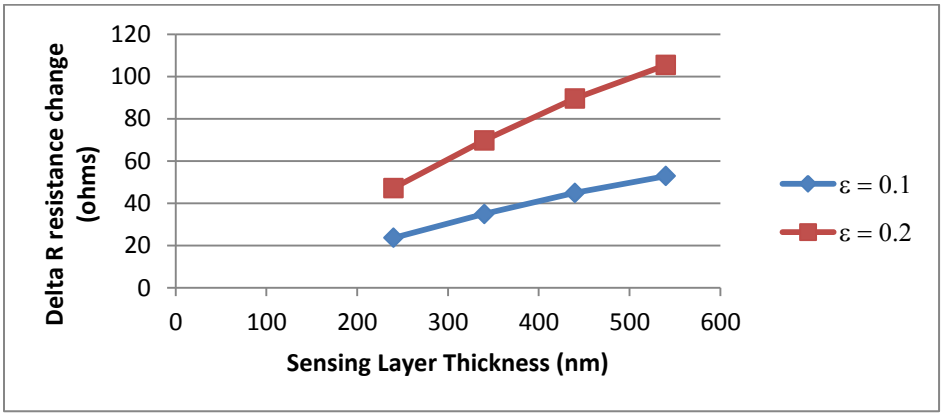

Figure 14: Plot of delta R as a function of sensing layer thickness for uniform chemically induced strain at back of cantilever at two different strain levels.

These can be compared to the effect of coating layer thickness on the front of the sensor listed in the table.

2.4 Different Material Sensing Layers

To model effect of indium or silver films of 340nm, thickness on the sensor response the different mechanical properties are entered in the model. In figure 5, bellow shows the delta resistance changes for coatings on the front and the back of the cantilever beam sensor for constant strain on 0.1%. In each case as the chemically induced strain is uniformly distributed in the film.

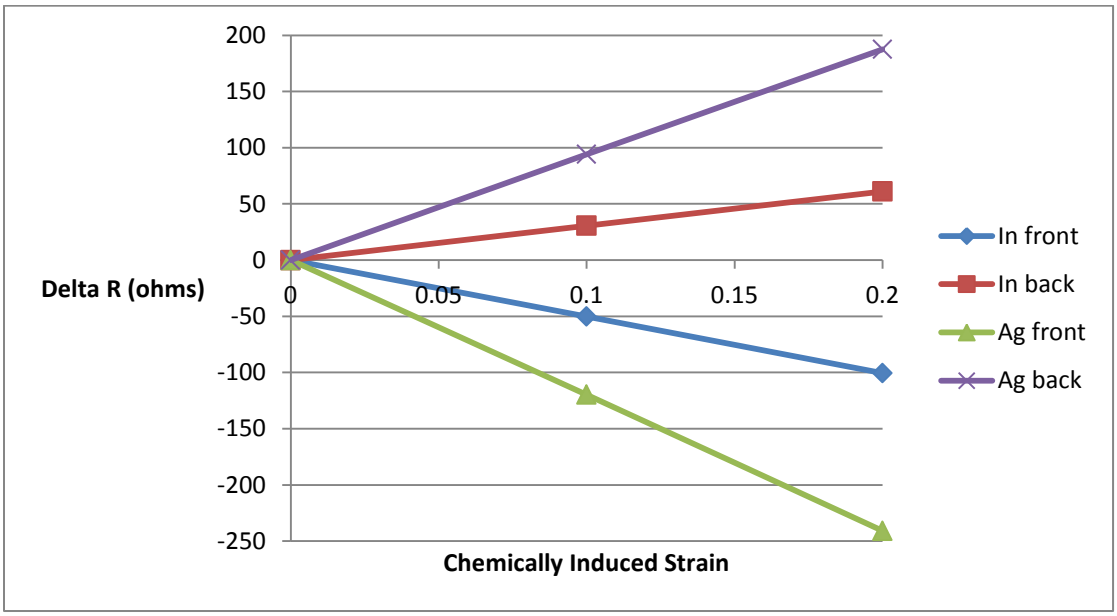

Figure 15: Plot of delta R as a function of chemically induced strain for different materials on front or back of sensor. (Note 340 nm silicon piezoresistive sensing layer thickness)

Effect of making piezoresistive sensor one half thickness has a significant effect on the resistance, actually doubling the value. To evaluate the sensitivity we must then divide by the zero strain resistance value in order to compare against the response with chemically induced strain. The normalized response is increased significantly for the thinner 170nm piezoresistive sensor, compared to the 340nm used in the experiments, with strain in the outermost half thickness of the sensing layer.

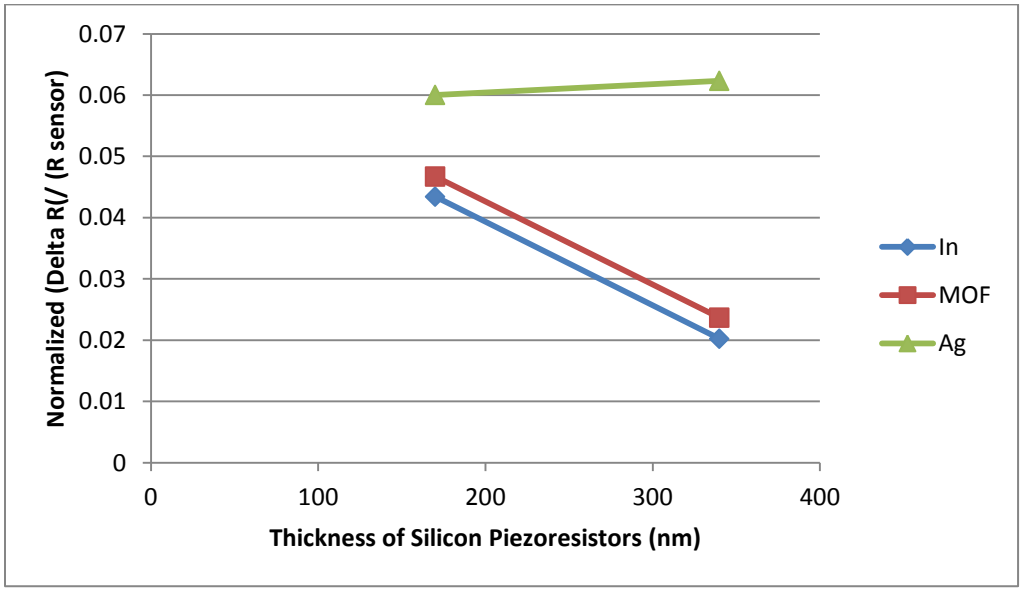

Figure 16: Plot of normalized sensitivity for 0.1% strain in full layer thick ness, as a function of piezoresistive silicon layer thickness, for different materials on the back of sensor.

Comparing the effect of silicon layer thickness for each of the coatings, the optimum layer thickness appears to be a function of the coating mechanical properties.

2.5 Response as a Function of Reacted Layer Thickness

Comparison for the strain induced in only 50% of film thickness, i.e. the outer layer of sensing film, for indium and silver coatings on the back of the sensor only, figure 7 and 8. Here the response is less than double for the full reacted layer, showing some nonlinear behavior as a function of thickness. The layer thickness which is reacted is a critical part of the response, as the unreacted portion adds stiffness to the beam lowering sensitivity. However the different response calculated as a function of silicon piezoresistive layer thickness indicated the responses are closer together and less dependent on the sensing layer mechanical properties. In particular for the In film the response is almost four times larger.

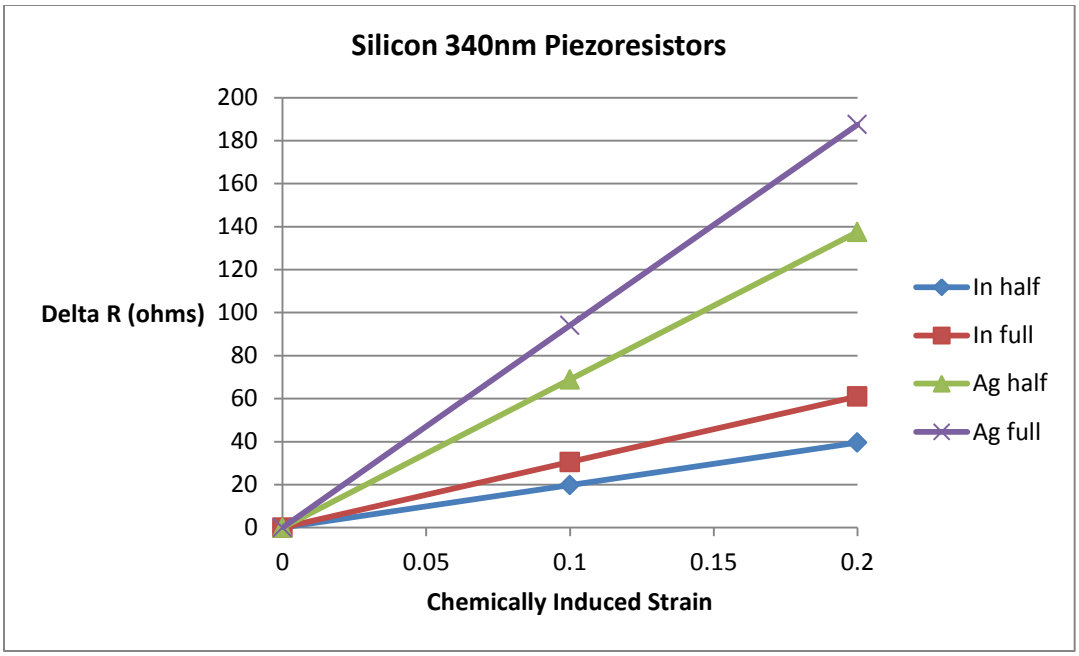

Figure 17: Plot of delta R as a function of chemically induced strain for different materials on back of sensor. (340nm thick silicon piezoresistive layer)

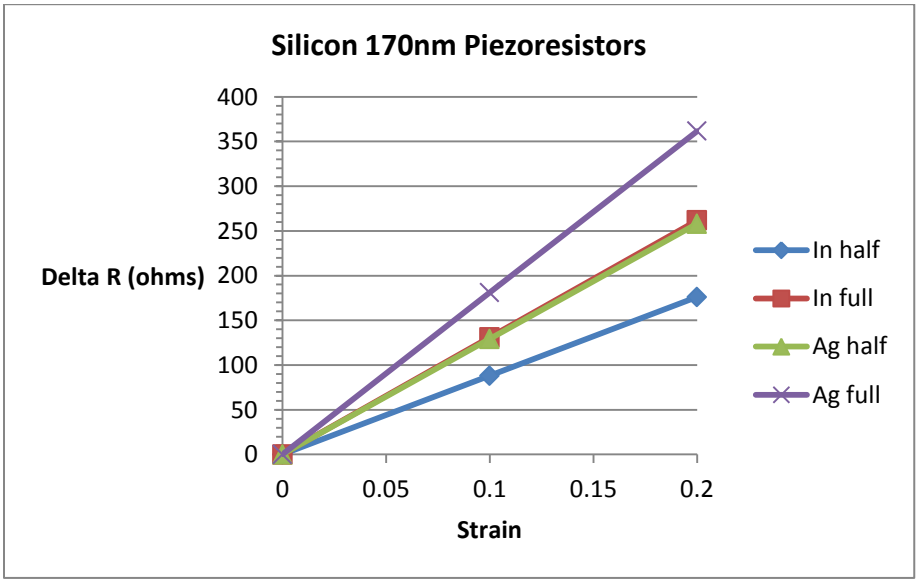

Figure 18: Plot of delta R as a function of chemically induced strain for different materials on back of sensor. (170nm thick silicon piezoresistive layer)

Comparing the effect of silicon layer thickness for each of the coatings, the sensitivity is improved with thinner silicon piezoresistive layers. This might be worth further investigation to examine the effect of width of the cantilever on response and placement of the silicon beam relative to the coating area and if the coating area in continuous or in a mosaic layer to distribute the stress.